Robotica (2016) volume 34, pp. 2653–2668. © Cambridge University Press 2015
doi:10.1017/S0263574715000272

Geometric design of planar mechanisms based on virtual guides for manipulation

Nina Robson†‡ and Shramana Ghosh‡*

†*Mechanical Engineering Department, California State University, Fullerton, California, USA*
‡*Mechanical and Aerospace Engineering Department, University of California, Irvine, California, USA*

(Accepted March 25, 2015. First published online: April 29, 2015)

SUMMARY
This paper presents recent results and applications of our planar kinematic synthesis of serial and parallel linkages to guide a rigid body, such that it does not violate normal direction and curvature constraints imposed by contact with objects in the environment. The paper briefly reviews the recently developed theory on transforming contact direction and curvature constraints into conditions on velocity and acceleration of certain points in the moving body to obtain synthesis equations which can, subsequently be solved to find the dimensions of a mechanical linkage. The main contribution of the paper is in demonstrating the applicability of the proposed theory to the kinematic synthesis of both open and closed-loop kinematic linkages. We provide preliminary results on the synthesis of kinematic chains based on novel task specifications that incorporate curvature constraints with a variety of applications, such as passive suspensions for small rovers, assistive technologies, as well as grasping.

KEYWORDS: Planar kinematic synthesis; Planar linkages; Higher-order constrained motion; Grasping; Assistive technology; Passive suspensions.

1. Introduction

This paper demonstrates the applicability of recent results in kinematic synthesis of planar mechanical chains that guide a workpiece, through specified positions such that they maintain contact with objects in their workspace. Robson and McCarthy[1] approach this problem by requiring the mechanical chain to be synthesized to match the contact force and curvature constraints imposed on the movement of the workpiece by contact with objects in the environment. Then the force and curvature constraints are transformed into conditions on the velocity and acceleration of certain points in the moving body. This gives a set of synthesis equations that allows the computation of design parameters of a chain that satisfies the contact force and curvature constraints imposed on the movement of the workpiece.

2. Literature Survey

Vafa and Dubowsky[2] introduced the concept of virtual manipulators for modeling manipulators working in space. Virtual Manipulators can be used to efficiently solve the inverse kinematic problem and calculate the workspace of space manipulators.

Rimon and Burdick[3,4] introduced the concept of second order mobility of a constrained body, and showed how the relative curvature of the surfaces in contact act to limit movement. Our goal is to consider how this viewpoint can be used to synthesize a linkage that guides a body such that it satisfies obstacle constraints. The approach to this problem is to use the relative curvature of the contact of an end-effector with one or more objects to define velocity and acceleration specifications for the movement of the end-effector. This provides kinematic constraints that can be used to synthesize the dimensions of the serial chain. The synthesis of planar linkages for velocity and acceleration

* Corresponding author. E-mail: shramang@uci.edu

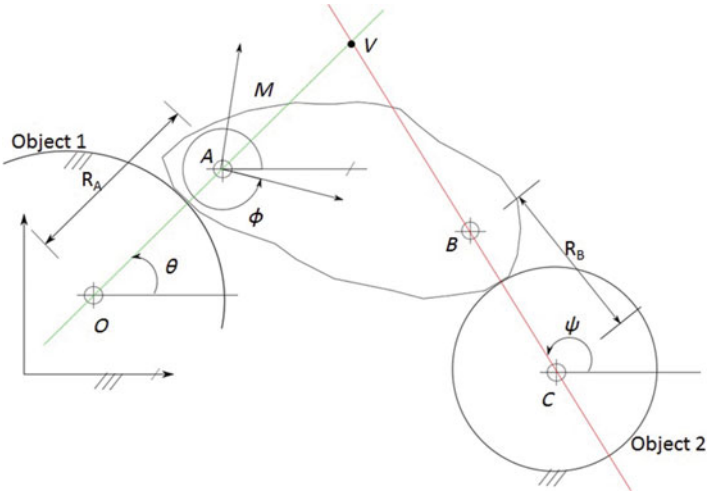

Fig. 1. The body M moves in contact with two objects such that the trajectories of $\boldsymbol{A}$ and $\boldsymbol{B}$ have the radii of curvature, R_A and R_B, respectively.

constraints was formulated about 40 years ago by Tesar[5] and Dowler, Duffy and Tesar.[6] The design equations for spatial SS chains for finitely and infinitesimally separated positions are found in Chen and Roth.[7] The case of seven finitely specified task positions is solved in Innocenti[8] and further studied by Liao and McCarthy.[9] Spherical movement, curvature theory, as well as instantaneous properties of trajectories, generated by planar, spherical and spatial motion has been discussed in McCarthy and Roth,[10,11] McCarthy,[12] recent details can be found in McCarthy[13,14] and Robson and McCarthy[1] and Robson and Tolety.[15]

This paper demonstrates how the developed synthesis theory with incorporated second order motion constraints can be used in the design process with the main goal of maintaining relative contact and curvature constraints between the moving body and objects in the environment.

3. Planar Contact Direction and Curvature

Let the movement of a rigid body be defined by the parameterized set of 3×3 homogeneous transforms $[T(t)] = [R(t), \boldsymbol{d}(t)]$ constructed from a rotation matrix, $R(t)$, and translation vector $\boldsymbol{d}(t)$. A point $\boldsymbol{p}$ fixed in the moving body traces a trajectory $\boldsymbol{P}(t)$ in a fixed coordinate frame F, given by

$$\begin{Bmatrix} P_x(t) \\ P_y(t) \\ 1 \end{Bmatrix} = \begin{bmatrix} \cos\phi(t) & -\sin\phi(t) & d_x(t) \\ \sin\phi(t) & \cos\phi(t) & d_y(t) \\ 0 & 0 & 1 \end{bmatrix} \begin{Bmatrix} p_x \\ p_y \\ 1 \end{Bmatrix}, \tag{1}$$

or

$$\boldsymbol{P}\,(t) = [T\,(t)]\,\boldsymbol{p}. \tag{2}$$

Our goal is to determine the movement $[T(t)]$ that has the property that two points in the moving body have the trajectories $\boldsymbol{A}(t)$ and $\boldsymbol{B}(t)$ consistent with contact with two circular virtual guides, Object 1 and Object 2, as shown Fig. 1.

Now position the coordinate frame M such that its origin coincides with $\boldsymbol{A}(t)$ and its x-axis is directed along the line $\boldsymbol{B} - \boldsymbol{A}$. This defines $[T(t)]$ with translation vector is $\boldsymbol{d}(t)$ and the rotation angle, $\phi(t)$ are given by

$$\boldsymbol{d}\,(t) = \boldsymbol{A}\,(t)\,, \phi\,(t) = \tan^{-1}\frac{\vec{k} \times (B - A)\,.\,(B - A)}{(B - A)\,.\,(B - A)}, \tag{3}$$

https://doi.org/10.1017/S0263574715000272 Published online by Cambridge University Press

where $\vec{k}$ is a vector perpendicular to the plane of movement. The vector $\vec{k}$ combines with the cross product operation to perform a 90° rotation in the plane, so for a vector $\boldsymbol{y}$, we have

$$\vec{k} \times \boldsymbol{y} = [J]\,\boldsymbol{y}, \;\; \textit{where}\; [J] = \begin{bmatrix} 0 & -1 \\ 1 & 0 \end{bmatrix}. \tag{4}$$

In what follows, we determine on the position, velocity and acceleration of the body at an instant denoted $t = 0$, from properties of the trajectories $\boldsymbol{A}(t)$ and $\boldsymbol{B}(t)$ imposed by contact with two objects.

3.1. The position, velocity and acceleration specifications

We assume that the contact of our moving body M with two fixed objects constrain the point trajectories $\boldsymbol{A}(t)$ and $\boldsymbol{B}(t)$ to follow circles in the vicinity of a reference position denoted by $t = 0$. The movement of M in the vicinity of $t = 0$ can be expressed as the Taylor series expansion,

$$[T\,(t)] = [T_0] + [T_1]\,t + \frac{1}{2}\,[T_2]\,t^2 + \cdots, \quad \textit{where}\;\; [T_i] = \frac{d^i\,[T]}{dt^i}. \tag{5}$$

Evaluating the derivatives of $[T(t)]$, we obtain

$$\begin{aligned}
[T_0] &= \begin{bmatrix} \cos\phi_0 & -\sin\phi_0 & d_{x,0} \\ \sin\phi_0 & \cos\phi_0 & d_{y,0} \\ 0 & 0 & 1 \end{bmatrix}, \\
[T_1] &= \begin{bmatrix} -\varphi_1 \sin\phi_0 & -\varphi_1 \cos\phi_0 & d_{x,1} \\ \varphi_1 \cos\phi_0 & -\varphi_1 \sin\phi_0 & d_{y,1} \\ 0 & 0 & 0 \end{bmatrix}, \\
[T_2] &= \begin{bmatrix} -\varphi_2 \sin\phi_0 - \varphi_1^2 \cos\phi_0 & -\varphi_2 \cos\phi_0 + \varphi_1^2 \sin\phi_0 & d_{x,2} \\ \varphi_2 \cos\phi_0 - \varphi_1^2 \sin\phi_0 & -\varphi_2 \sin\phi_0 - \varphi_1^2 \cos\phi_0 & d_{y,2} \\ 0 & 0 & 0 \end{bmatrix}.
\end{aligned} \tag{6}$$

We have introduced the notation $d^i\phi/dt^i(0) = \phi_i$ and $d^i\boldsymbol{d}/dt^i(0) = \left(d_{x,i}, d_{y,i}\right)^T = \boldsymbol{d}_i$.

The data provided for the position of the moving frame M identifies the coordinates of the contact points $\boldsymbol{A_0} = \boldsymbol{A}(0)$ and $\boldsymbol{B_0} = \boldsymbol{B}(0)$, so we have

$$\boldsymbol{d_0} = \boldsymbol{A_0}, \phi_0 = \tan^{-1} \frac{\vec{k} \times (\boldsymbol{B_0} - \boldsymbol{A}_0)\,.\,(\boldsymbol{B_0} - \boldsymbol{A_0})}{(\boldsymbol{B_0} - \boldsymbol{A}_0)\,.\,(\boldsymbol{B_0} - \boldsymbol{A_0})}, \tag{7}$$

This defines the coordinate transformation $[T_0]$.

In order to satisfy the force constraints at the prescribed positions, we determine directions of the velocities vectors $\dot{\boldsymbol{A}}$ and $\dot{\boldsymbol{B}}$ that are perpendicular to the forces $\boldsymbol{F_A}$ and $\boldsymbol{F_B}$. This is achieved by defining the point of intersection $\boldsymbol{V}$ of the lines of actions of these two forces (Fig. 1), and ensuring that it is the velocity pole of the movement of M in this position.

Let the angular velocity of M be defined as $\boldsymbol{w} = \dot{\phi}\vec{k}$, then $\boldsymbol{A}$ and $\boldsymbol{B}$ follow circles around $\boldsymbol{O}$ and $\boldsymbol{C}$, respectively. In this configuration, it is known that the point of intersection of the lines of action L_A^i and L_B^i of the constraint forces $\boldsymbol{F_A^i}$ and $\boldsymbol{F_B^i}$, is the velocity pole, $\boldsymbol{V}$ of the body and has zero velocity. The point $\boldsymbol{V}$ is obtained by simultaneous solution of the two linear equations

$$\begin{aligned}
L_A^i &: \left(\boldsymbol{V} - \boldsymbol{A^i}\right) \cdot [J]\,\boldsymbol{F_A^i} = 0, \\
L_B^i &: \left(\boldsymbol{V} - \boldsymbol{B^i}\right) \cdot [J]\,\boldsymbol{F_B^i} = 0, \quad i = 1, 2,
\end{aligned} \tag{8}$$

where $\boldsymbol{V} = (x, y)$ are variable point coordinates.

This allows us to determine the velocities of $\boldsymbol{A}$ and $\boldsymbol{B}$ considered as points in M, as

$$\dot{\boldsymbol{A}} = \boldsymbol{w} \times (\boldsymbol{A} - \boldsymbol{V}), \;\; \text{and}\; \dot{\boldsymbol{B}} = \boldsymbol{w} \times (\boldsymbol{B} - \boldsymbol{V}). \tag{9}$$

https://doi.org/10.1017/S0263574715000272 Published online by Cambridge University Press

The angular velocities $\boldsymbol{w}_{\boldsymbol{OA}} = \dot{\theta}\vec{k}$ and $\boldsymbol{w}_{\boldsymbol{CB}} = \dot{\psi}\vec{k}$ can be obtained from the relations

$$\begin{aligned} \dot{\boldsymbol{A}} &= \boldsymbol{w}_{OA} \times (\boldsymbol{A} - \boldsymbol{O}), \text{ and} \\ \dot{\boldsymbol{B}} &= \boldsymbol{w}_{CB} \times (\boldsymbol{B} - \boldsymbol{C}). \end{aligned} \tag{10}$$

We collect these results into the velocity loop equations of the quadrilateral $\boldsymbol{OABC}$, to compute the velocity $\boldsymbol{B} = \dot{\boldsymbol{A}} + \boldsymbol{w} \times (\boldsymbol{B} - \boldsymbol{A})$ to be

$$\boldsymbol{w}_{OA} \times (\boldsymbol{A} - \boldsymbol{O}) + \boldsymbol{w} \times (\boldsymbol{B} - \boldsymbol{A}) = \boldsymbol{w}_{CB} \times (\boldsymbol{B} - \boldsymbol{C}). \tag{11}$$

The angular velocity $\phi_1 = \dot{\phi}(0)$ and the velocity $\boldsymbol{d}_1 = \dot{\boldsymbol{A}}(0)$ define the elements of the velocity matrix $[T_1]$.

As the body M moves in contact with two objects, the points A and B are guided along trajectories with radii of curvature R_A and R_B. This is equivalent to the specification of points $\boldsymbol{O}$ and $\boldsymbol{C}$ which are the centers of curvature of the trajectories $\boldsymbol{A}(t)$ and $\boldsymbol{B}(t)$ at the instant $t = 0$.

We use the acceleration loop equations of the quadrilateral $\boldsymbol{OABC}$, in order to determine the angular accelerations $\boldsymbol{a}_{\boldsymbol{OA}} = \ddot{\theta}\vec{k}$ and $\boldsymbol{a}_{\boldsymbol{CB}} = \ddot{\psi}\vec{k}$ for a given value of the angular acceleration $\boldsymbol{a} = \ddot{\phi}\vec{k}$. This in turn allows us to determine $\ddot{\boldsymbol{d}} = \ddot{\boldsymbol{A}}$.

The acceleration loop equations are obtained by computing the time derivative of the velocity loop Eq. (11) to obtain

$$\begin{aligned} &\boldsymbol{a}_{OA} \times (\boldsymbol{A} - \boldsymbol{O}) + \boldsymbol{w}_{OA} \times (w_{OA} \times (\boldsymbol{A} - \boldsymbol{O})) \\ &\quad + \boldsymbol{a} \times (\boldsymbol{B} - \boldsymbol{A}) + \boldsymbol{w} \times (\boldsymbol{w} \times (\boldsymbol{B} - \boldsymbol{A})) \\ &\quad = \boldsymbol{a}_{CB} \times (\boldsymbol{B} - \boldsymbol{C}) + \boldsymbol{w}_{CB} \times (\boldsymbol{w}_{CB} \times (\boldsymbol{B} - \boldsymbol{C})). \end{aligned} \tag{12}$$

We now specify the angular acceleration of the moving body M to be $\ddot{\phi} = 0$, so $\boldsymbol{a} = 0$, and obtain the acceleration loop equations in the form

$$\begin{aligned} &\ddot{\theta}\vec{k} \times (\boldsymbol{A} - \boldsymbol{O}) - \dot{\theta}^2(\boldsymbol{A} - \boldsymbol{O}) - \dot{\phi}^2(\boldsymbol{B} - \boldsymbol{A}) \\ &\quad = \ddot{\psi}\vec{k} \times (\boldsymbol{B} - \boldsymbol{C}) - \dot{\psi}^2(\boldsymbol{B} - \boldsymbol{C}), \end{aligned} \tag{13}$$

which are simplified using the identity, $\vec{k} \times (\vec{k} \times \boldsymbol{y}) = -\boldsymbol{y}$. The angular acceleration $\ddot{\theta}$ is obtained by taking the dot product of Eq. (13) with $\boldsymbol{B} - \boldsymbol{C}$ to cancel the term containing $\ddot{\psi}$, that is

$$\ddot{\theta} = \frac{\left(\dot{\theta}^2 (\boldsymbol{A} - \boldsymbol{O}) + \dot{\phi}^2 (\boldsymbol{B} - \boldsymbol{A}) - \dot{\psi}^2 (\boldsymbol{B} - \boldsymbol{C})\right) \cdot (\boldsymbol{B} - \boldsymbol{C})}{\vec{k} \times (\boldsymbol{A} - \boldsymbol{O}) \cdot (\boldsymbol{B} - \boldsymbol{C})}. \tag{14}$$

In a similar way, we obtain $\ddot{\psi}$ by computing the dot product of Eq. (13) with $\boldsymbol{A} - \boldsymbol{O}$,

$$\ddot{\psi} = \frac{-\left(\dot{\theta}^2 (\boldsymbol{A} - \boldsymbol{O}) + \dot{\phi}^2 (\boldsymbol{B} - \boldsymbol{A}) - \dot{\psi}^2 (\boldsymbol{B} - \boldsymbol{C})\right) \cdot (\boldsymbol{A} - \boldsymbol{O})}{\vec{k} \times (\boldsymbol{B} - \boldsymbol{C}) \cdot (\boldsymbol{A} - \boldsymbol{O})}. \tag{15}$$

The result is a specification of the acceleration $\ddot{\boldsymbol{A}}$, given by

$$\ddot{\boldsymbol{A}} = \ddot{\theta}\vec{k} \times (\boldsymbol{A} - \boldsymbol{O}) - \dot{\theta}^2 (\boldsymbol{A} - \boldsymbol{O}). \tag{16}$$

Thus, the values $\phi_2 = 0$ and $d_2 = \ddot{\boldsymbol{A}}(0)$ determine the elements of the acceleration matrix $[T_2]$.

3.2. Relative movement

For convenience in what follows, we introduce the relative transformation $[D(t)] = [T(t)][T_0]^{-1}$ that operates on point coordinates measured in the fixed frame at the instant $t = 0$. Recall that a point

https://doi.org/10.1017/S0263574715000272 Published online by Cambridge University Press

$\boldsymbol{p}$ in M has the trajectory $\boldsymbol{P}(t)$ defined by the equation

$$\boldsymbol{P}(t) = [T(t)]\,\boldsymbol{p} = \left[T_0 + T_1 t + \frac{1}{2}T_2 t^2 + \ldots\right]\boldsymbol{p}. \tag{17}$$

Now let $\boldsymbol{P} = [T_0]\boldsymbol{p}$, then we have

$$\begin{aligned}\boldsymbol{P}(t) &= \left[T_0 + T_1 t + \frac{1}{2}T_2 t^2 + \cdots\right][T_0]^{-1}\,\boldsymbol{P},\\ &= \left[I + \Omega t + \frac{1}{2}\Lambda t^2 + \cdots\right]\boldsymbol{P} = [D(t)]\,\boldsymbol{P},\end{aligned} \tag{18}$$

where

$$\begin{aligned}[\Omega] &= \begin{bmatrix} 0 & -\phi_1 & d_{x,1} + d_{y,0}\theta_1 \\ \phi_1 & 0 & d_{y,1} - d_{x,0}\theta_1 \\ 0 & 0 & 0 \end{bmatrix},\\ [\Lambda] &= \begin{bmatrix} -\phi_1^2 & -\phi_2 & d_{x,2} + d_{x,1}\phi_1^2 + d_{y,0}\phi_2 \\ \phi_2 & -\phi_1^2 & d_{y,2} + d_{y,1}\phi_1^2 + d_{x,0}\phi_2 \\ 0 & 0 & 0 \end{bmatrix},\end{aligned} \tag{19}$$

are the velocity and acceleration matrices. In the following section, we use this formulation of the movement of M to describe the trajectory of a general point $\boldsymbol{P}(t)$.

4. The Synthesis Equations for a Planar RR Serial Chain for Contact and Curvature Task Constraints

As mentioned above, we determine the movement of M such that its position, velocity and acceleration are known in one location, and its position and velocity are known in a second location. This implies that contact curvatures are specified in the first location and constraint forces in the second location. We start by obtaining the movement $[T(t)]$, that has the property that two points in the moving body have the trajectories $\boldsymbol{A}(t)$ and $\boldsymbol{B}(t)$, consistent with contact with two circular objects in each of the two positions. We define our task, by determining the position, velocity and acceleration of the body at an instant $t = 0$, from properties of the trajectories $\boldsymbol{A}(t)$ and $\boldsymbol{B}(t)$ imposed by contact with the two objects.

Next, we formulate the design equations of a planar RR chain for a task that includes contact with the environment. The chain has five design parameters the coordinates of the fixed pivot $\boldsymbol{G} = (u, v, 1)$ in the fixed frame F, the coordinates of the moving pivot $\boldsymbol{w}$ in the moving frame M, and the length of the crank R.

The geometry of the RR chain satisfies the constraint equation

$$(\boldsymbol{W} - \boldsymbol{G}) \cdot (\boldsymbol{W} - \boldsymbol{G}) = R^2, \tag{20}$$

where $\boldsymbol{W}$ defines the fixed frame coordinates of the moving pivot $\boldsymbol{w}$. The first and second derivatives of this equation yield the additional constraint equations

$$\begin{aligned}\dot{\boldsymbol{W}} \cdot (\boldsymbol{W} - \boldsymbol{G}) &= 0,\\ \ddot{\boldsymbol{W}} \cdot (\boldsymbol{W} - \boldsymbol{G}) + \dot{\boldsymbol{W}} \cdot \dot{\boldsymbol{W}} &= 0.\end{aligned} \tag{21}$$

To use these equations for designing the RR chain, we specify the movement of M, so we have the $\boldsymbol{W}(t) = [T(t)]\boldsymbol{w}$. The resulting equations can be solved algebraically to determine the design parameters.[6]

https://doi.org/10.1017/S0263574715000272 Published online by Cambridge University Press

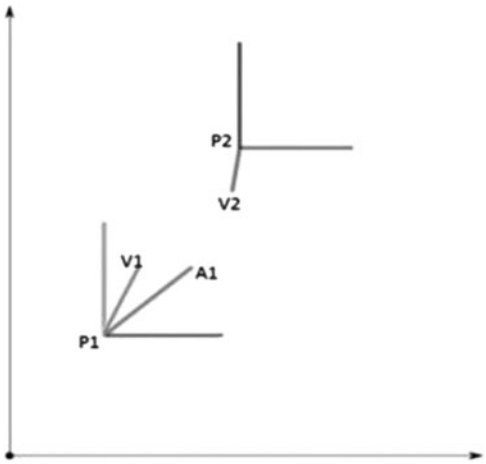

Fig. 2. Planar Task: Example of a five multiply separated position task. It consists of two positions, two velocities (implying normal direction constraints at the two positions), and an acceleration at the first position (giving curvature constraint at that position).

4.1. The design equations

Five design equations for the RR chain are obtained by determining the movement of M such that its position, velocity and acceleration are known in one location, and its position and velocity are known in a second location. From our previous results, this implies that contact curvatures are specified in the first location and constraint forces in the second location. Thus, the matrix functions

$$\begin{aligned} [T^1(t)] &= [T_0^1] + [T_1^1] + \tfrac{1}{2}\left[T_2^1\right] t^2, \\ \left[T^2(t)\right] &= \left[T_0^2\right] + \left[T_1^2\right] t, \end{aligned} \tag{22}$$

where $[T_0^j]$, $[T_1^j]$, $j = 1, 2$ and $[T_2^1]$, are known.

In what follows, it is convenient to use the coordinate of the moving pivot in the first location $\boldsymbol{W}^1 = (x, y, 1)$ as design parameters for the RR chain, rather than the moving pivot coordinates $\boldsymbol{w}$ in M, where $\boldsymbol{W}^1 = [T_0^1]\boldsymbol{w}$.

This allows us to define the trajectories $W^1(t)$ and $\boldsymbol{W}^2(t)$ using the relative displacement matrices defined in Eqs. (18) and (19), so we have

$$\begin{aligned} \boldsymbol{W}^1(t) &= \left[D^1(t)\right] \boldsymbol{W}^1 = \left[I + \Omega^1 t + \frac{1}{2}\Lambda^1 t^2\right] \boldsymbol{W}^1 \\ \boldsymbol{W}^2(t) &= \left[D^2(t)\right] \boldsymbol{W}^2 = \left[I + \Omega^2 t\right] [D_{12}]\, \boldsymbol{W}^1, \end{aligned} \tag{23}$$

where $[D_{12}] = [T_0^2][T_0^1]^{-1}$. This yields $\boldsymbol{W}^2 = [D_{12}]\, \boldsymbol{W}^1$. Substitute the trajectories Eq. (23) into the constraint Eqs. (20) and (21) to obtain,

$$\begin{aligned} \wp_1 : 0 &= \left(\boldsymbol{W}^1 - \boldsymbol{G}\right) \cdot \left(\boldsymbol{W}^1 - \boldsymbol{G}\right) - R^2 \\ \mathcal{V}_1 : 0 &= \left[\Omega^1\right] \boldsymbol{W}^1 \cdot \left(\boldsymbol{W}^1 - \boldsymbol{G}\right) \\ \mathcal{A}_1 : 0 &= \left[\Lambda^1\right] \boldsymbol{W}^1 \cdot \left(\boldsymbol{W}^1 - \boldsymbol{G}\right) + \left[\Omega^1\right] \boldsymbol{W}^1 \cdot \left[\Omega^1\right] \boldsymbol{W}^1 \\ \wp_2 : 0 &= \left([D_{12}]\, \boldsymbol{W}^1 - \boldsymbol{G}\right) \cdot \left([D_{12}]\, \boldsymbol{W}^1 - \boldsymbol{G}\right) - R^2 \\ \mathcal{V}_2 : 0 &= \left[\Omega^2\right] [D_{12}]\, \boldsymbol{W}^1 \cdot \left([D_{12}]\, \boldsymbol{W}^1 - \boldsymbol{G}\right). \end{aligned} \tag{24}$$

These are the design equations for the RR chain. An example of a planar task, consisting of positions and higher order derivatives can be seen in Fig. 2.

4.2. Trajectory planning

The inverse kinematics of the RR chain yields the joint parameter vector $\boldsymbol{q} = (\theta_1, \theta_2)$ at each of the task positions, $i = 1, 2$. In order to obtain the joint velocity vector $\dot{\boldsymbol{q}}$ at the ith position, we solve the

https://doi.org/10.1017/S0263574715000272 Published online by Cambridge University Press

equation

$$V_i = [J_i]\,\dot{\boldsymbol{q}}_{\boldsymbol{i}} \quad i = 1, 2, \tag{25}$$

where $V_i = (\omega, \boldsymbol{v})$ is the velocity prescribed at position i, and J_i is the Jacobian of the RR chain. Notice that the Jacobian is a 3×2 matrix, and the solution is obtained by pre-multiplying by the inverse of the Jacobian

$$\dot{\boldsymbol{q}}_{\boldsymbol{i}i} = \left[J_i^T J_i\right]^{-1}\left[J_i^T\right] V_i, \quad i = 1, 2. \tag{26}$$

This is the well-known pseudo-inverse which provides an exact solution because the linkage was designed to satisfy this velocity requirement.

Now to determine the joint acceleration vector $\ddot{\boldsymbol{q}}$, we solve the equation

$$A_i = \dot{J}_i \dot{\boldsymbol{q}}_{\boldsymbol{i}} + J_i \ddot{\boldsymbol{q}}_{\boldsymbol{i}}, \quad i = 1, \tag{27}$$

where $A_i = (\alpha, \boldsymbol{a})$ is the acceleration prescribed at the first position and $\dot{J}_i$ is the time derivative of the 3×2 Jacobian matrix. The vector $\dot{J}_i \dot{\boldsymbol{q}}_i$ is known so we can subtract it from both sides, thus the solution is obtained using the pseudo-inverse,

$$\ddot{\boldsymbol{q}}_{\boldsymbol{i}} = \left[J_i^T J_i\right]^{-1}\left[J_i^T\right]\left(A_i - \dot{J}_i \dot{\boldsymbol{q}}_{\boldsymbol{i}}\right). \tag{28}$$

The trajectory between the joint parameters $(\theta_0, \dot{\theta}_0, \ddot{\theta}_0)$ and $(\theta_f, \dot{\theta}_f, \ddot{\theta}_f)$ over the range $0 \le t \le t_f$ is generated by the fifth degree polynomial

$$\theta(t) = a_0 + a_1 t + a_2 t^2 + a_3 t^3 + a_4 t^4 + a_5 t^5, \tag{29}$$

where

$$a_0 = \theta_0, \quad a_1 = \dot{\theta}_0, \quad a_2 = \frac{\ddot{\theta}_0}{2},$$

$$a_3 = \frac{20\theta_f - 20\theta_0 - \left(8\dot{\theta}_f + 12\dot{\theta}_0\right) t_f - \left(3\ddot{\theta}_0 - \ddot{\theta}_f\right) t_f^2}{2t_f^3},$$

$$a_4 = \frac{30\theta_0 - 30\theta_f + \left(14\dot{\theta}_f + 16\dot{\theta}_0\right) t_f + \left(3\ddot{\theta}_0 - 2\ddot{\theta}_f\right) t_f^2}{2t_f^4},$$

$$a_5 = \frac{12\theta_f - 12\theta_0 - \left(6\dot{\theta}_f + 6\dot{\theta}_0\right) t_f - \left(\ddot{\theta}_0 - \ddot{\theta}_f\right) t_f^2}{2t_f^5}.$$

Equation (29) is obtained by solving the equations defining the joint position, velocity and acceleration evaluated at $t = 0$ and $t = t_f$ to compute the coefficients $a_i, i = 0, \ldots, 5$ (see Eq. 26).

5. Synthesis of Planar Mechanisms Based on Virtual Guides for Manipulation

5.1. Design of a two-bar passive lower extremity device for people with below knee injuries

In order to resolve the disadvantages of conventional crutch designs (i.e. underarm and forearm), a novel crutch design is developed. Prior to the design, human natural treadmill walking was monitored by a 3D motion capture system and a reference end-foot trajectory was obtained (see Fig. 3). The walking motion can be assumed as a planar task on the sagittal plane, which consists of positioning the foot, at the point, $M_j (j = 1, \cdots, n)$, located on the reference trajectory. If the kinematic specifications at the start (i.e. heel strike) and end points (i.e. toe off) are acquired, it is possible to synthesize an

https://doi.org/10.1017/S0263574715000272 Published online by Cambridge University Press

Table I. Task data for the synthesis of a planar RR chain. The angles are measured in radians, the position data is given in units, where 1unit = 20 cm.

Posit	$(\phi,\ \boldsymbol{d}_x,\ \boldsymbol{d}_y)$	Vel. Data	Accel. Data
1	(0, 2.2, 1.414)	(1, 0.532, 2.088)	(0, 1.181, 4.631)
2	(0, 4.5, 1.3)	(1, 0.655, −2.153)	—

Table II. The two real solutions (1unit = 20 cm) from the synthesis of the RR chain. The first solution has been used in the design of the passive leg.

Solution	G = (*u*, *v*)	W = (*x*, *y*)
1	(2.919, 4.736)	(1.706, 3.532)
2	(−1.3365, 1.911)	(−2.519, 1.884)

RR chain to mimic the reference trajectory pattern. The velocity and acceleration specifications are derived from the curvature information in the two positions and are compatible with contact and curvature constraints between the foot and the ground. The synthesis task is listed in Table I.

The leg was synthesized as an RR planar kinematic chain where the first hinge joint is located at the hip and the other hinge joint at the knee and animated in Mathematica. Figure 3 presents results on the design of a simple RR passive lower extremity device for people with leg injury, based on the natural walking gait foot trajectory. The synthesis solutions for the RR chain are obtained from design Eq. (24) and are shown in Table II.

Based on the design results, two different types of passive walking prototypes, consisting of a self-retracting knee-joints were fabricated, one at Texas A&M University (TAMU) and the other one at California State University, Fullerton (CSUF). The devices and their end-foot trajectories are given in Figs. 4, 5 and 6.

The performance of both devices was tested by 2 mph treadmill walking. Because of the specified acceleration in the first position, both synthesized devices show satisfactory performance. The CSUF design, shown in Figs. 5 and 6, incorporates an additional cam-type of joint at the hip level and demonstrates better performance in obtaining the desired natural "tear-drop" shape trajectory at the end of the foot.

5.2. Design of a planar six bar passive suspension for a rover platform, capable of operating in challenging environments

A novel passive suspension design based on contact and curvature specifications of the wheel with objects in the environment is shown in Fig. 7. The example is a part of our efforts on developing autonomous robot systems operating in remote and challenging environments. This novel type of suspension incorporates two four-bar linkages and was designed with the main goal of being having a climbing capacity of more than two times the wheel diameter.

In four-wheel drive vehicles, obstacle limit is generally half of the wheel diameter. It is possible to pass over this height by pushing the driving wheel to the obstacle, which is called climbing. For this condition, the contact point of the wheel and obstacle is at the same height with the wheel center. Although obstacle geometries can vary, the most difficult geometry which can be climbed by a wheeled vehicle is a stair-type rectangular obstacle. Tests show that Mars rover is able to overcome about 1.5 times the height of its wheel diameter. This limitation forces scientists to improve their current designs. In addition, if the surface friction of an obstacle is not enough to climb, the obstacle force on the wheel can reach high values. A solution for this problem is the use of a linear motion suspension where obstacle reaction force cannot create any moment.

The climbing motion in our case consist of two sub-motions. The first one is a vertical motion which causes a horizontal reaction force on the wheel center. The vertical motion instant center is at infinity. The second sub-motion is a soft rotation about a point located at the top of an obstacle, with an instant center of rotation at that point. We define a start and an end position, located at the start of a step and at the step corner/edge, respectively, and use velocity and acceleration task specifications

https://doi.org/10.1017/S0263574715000272 Published online by Cambridge University Press

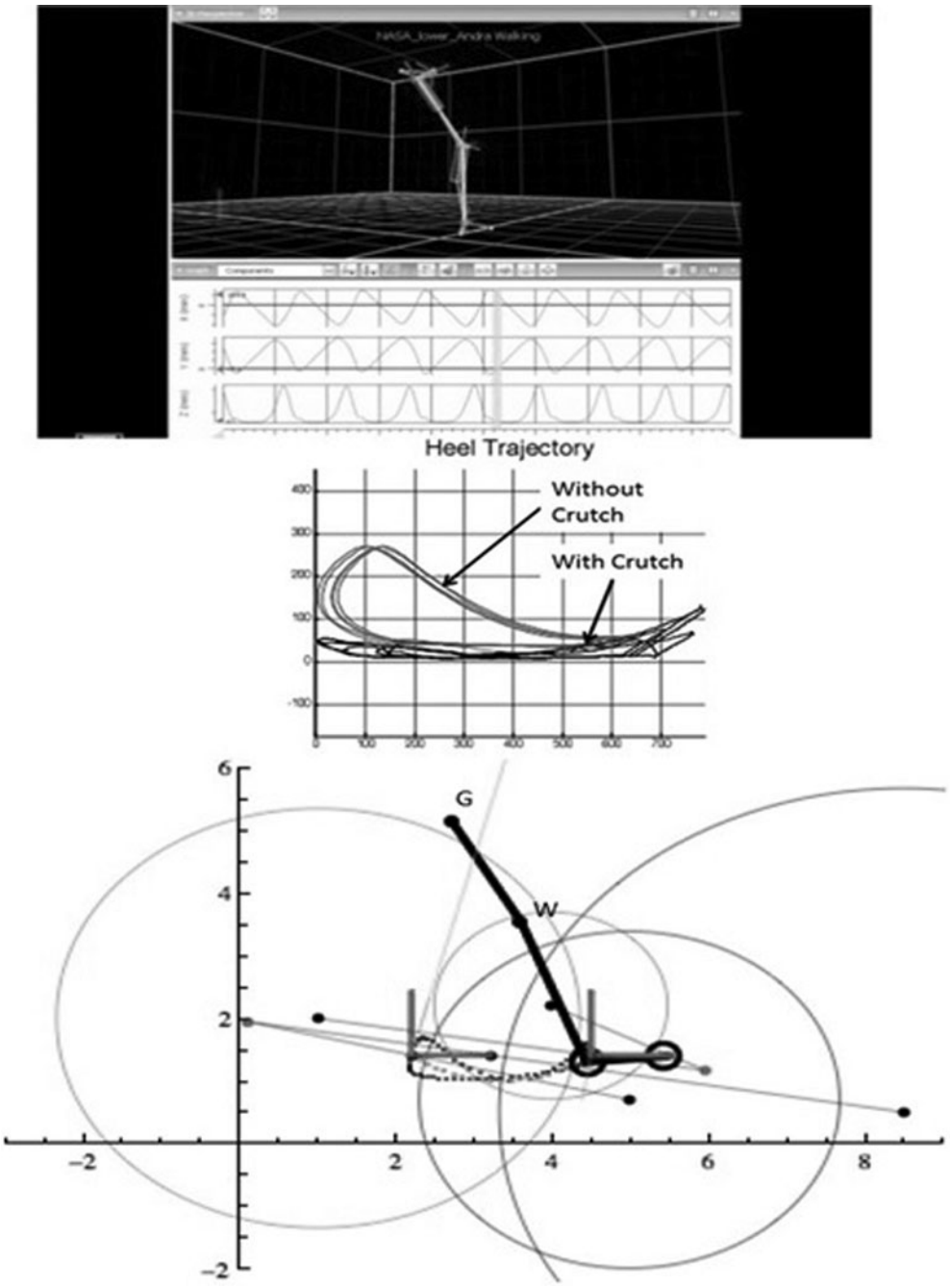

Fig. 3. Natural walking gait cycle trajectories at foot level obtained from Vicon motion capture system (up). An RR planar kinematic chain is synthesized based on that trajectory (down). Due to the contact and curvature specifications in the vicinity of the first position, the RR chain still follows the curvature of the virtual obstacles.

defined in the two positions. These velocities and accelerations are directly derived from the geometry of the problem, and are compatible with contact and curvature constraints of the wheels with objects in the environment (see Table III).

After the task has been specified, the dimensions of the chain, which satisfy the task specifications is calculated. The goal for our kinematic synthesis is to calculate the design parameters for the linkage suspension that accounts for the physical contact of the wheel with an obstacle in the workspace during the motion. A four-bar linkage has been synthesized to obtain the desired straight-line motion of the wheel center. The synthesis results are given in Table IV.

https://doi.org/10.1017/S0263574715000272 Published online by Cambridge University Press

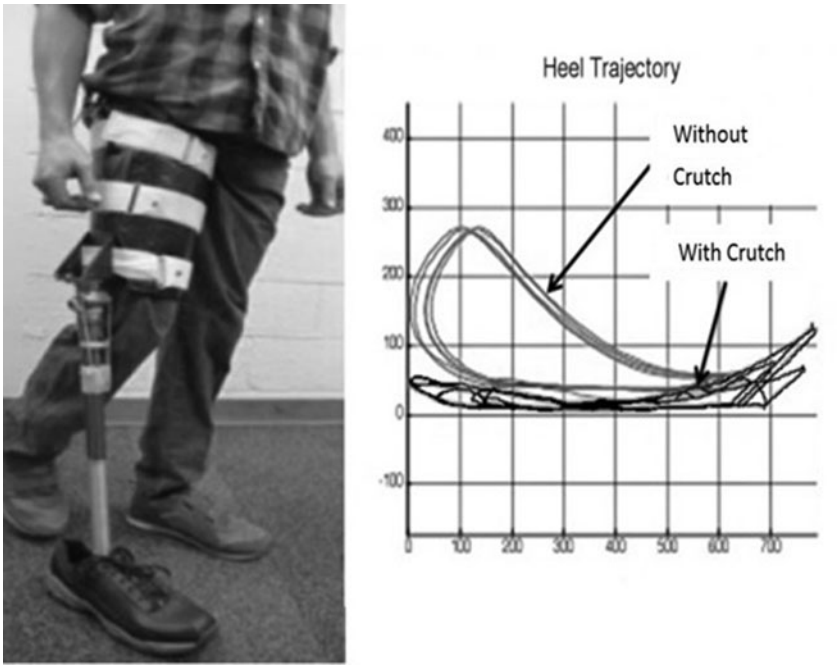

Fig. 4. Prototype of the passive assistive walking device for a lower leg injury, developed at TAMU.

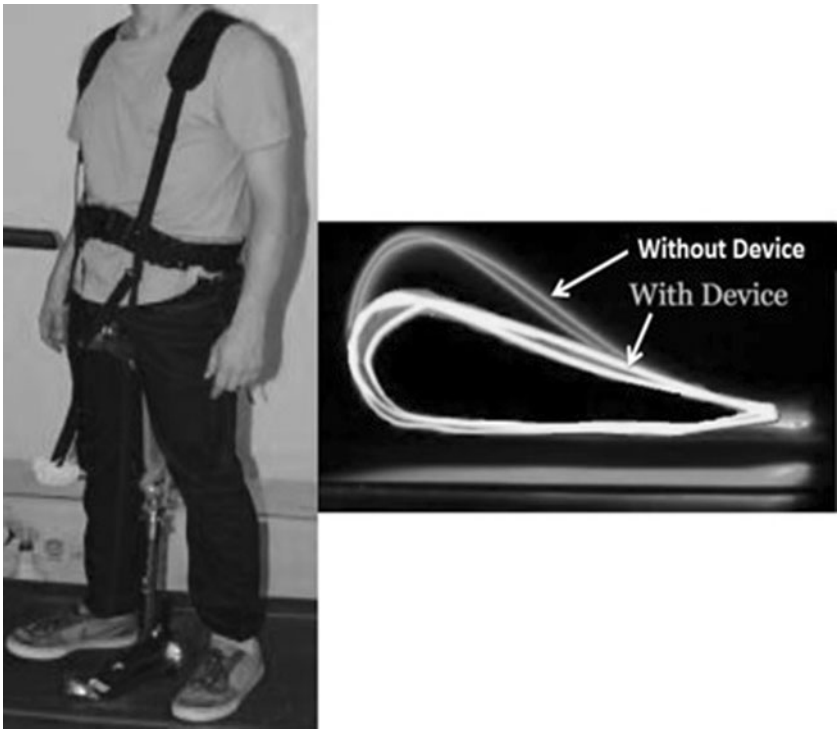

Fig. 5. The end-foot trajectory of a person, walking with the passive assistive walking device for a lower leg injury, developed at CSUF.

As a next step, the suspension is constructed by connecting two four-bar linkages symmetrically, where one of the four-bar linkages is a mirror image of the other. Figures 7 and 8 show the chosen design that best fits the requirements, based on climbing capacity of about three times the wheel diameter, and its linear ratio of 0.10, which indicates the ratio of $x_{\max}$ displacement over the total y displacement of the wheel from the ground. The prototype of the rover is shown in Fig. 9.

https://doi.org/10.1017/S0263574715000272 Published online by Cambridge University Press

Fig. 6. The end-foot trajectory of a person, walking with the passive assistive walking device for a lower leg injury, developed at CSUF.

Table III. Task data for the synthesis of a planar RR chain. The angles are measured in radians, the position data is given in units, where 1unit = 5 cm.

Posit	$(\phi,\ \boldsymbol{d_x},\ \boldsymbol{d_y})$	Vel. Data	Accel. Data
1	(0, 3.2, 2.401)	(1, 0.782, 1.869)	(0, 1.952, 4.665)
2	(0, 3.5, 7.2)	(1, −0.2, 0)	–

Table IV. The two real solutions (1unit = 5 cm) from the synthesis of the RR chain are gathered together to obtain a one degree of freedom four bar linkage.

Solution	G = (*u*, *v*)	W = (*x*, *y*)
1	(−0.261, 6.864)	(−0.051, 4.099)
2	(−1.323, 0.397)	(−2.296, −0.653)

5.3. Design of one degree of freedom robotic fingers based on anthropometric data and anthropomorphic tasks

This subsection shows our recent efforts on using second order task constraints for the kinematic synthesis and design of mechanical fingers and hands. Here, we describe a method for the kinematic synthesis of one degree-of-freedom robotic fingers that incorporate multi-loop kinematic structures with second order task specifications, such that the fingers do not violate normal direction and curvature constraints imposed by contact with objects. We show how to use these contact and curvature effects to formulate the synthesis equations for the design of a planar thumb and index fingers, based on anthropometric back-bone chain and anthropomorphic task.

A one degree-of-freedom planar four-bar and eight-bar linkages are considered for our mechanical thumb and index finger, respectively. The four-bar linkage thumb has been chosen due to its particular topology and the eight-bar linkage is chosen due to the flexibility it has for choosing the ground pivot locations[16] and its grasping performance. Our goal is to design linkage-based mechanisms that incorporate higher order motion constraints to mimic human grasping operation. To design such devices, we first obtain kinematic data (position, velocity, acceleration) of a subject performing a grasping task using both a sensor based glove[17,18] and a 3D motion capture system (Fig. 10). The glove is equipped with MEMS based accelerometers at the fingertips and infrared markers to give

https://doi.org/10.1017/S0263574715000272 Published online by Cambridge University Press

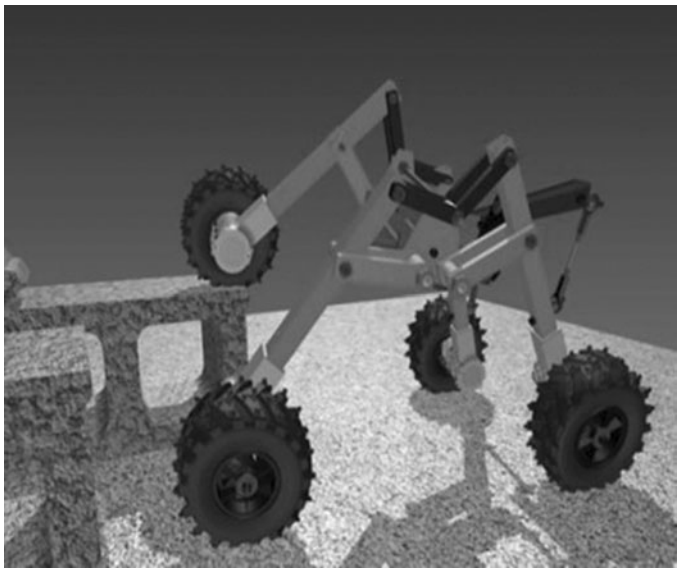

Fig. 7. CAD drawing of the passive rover suspension.

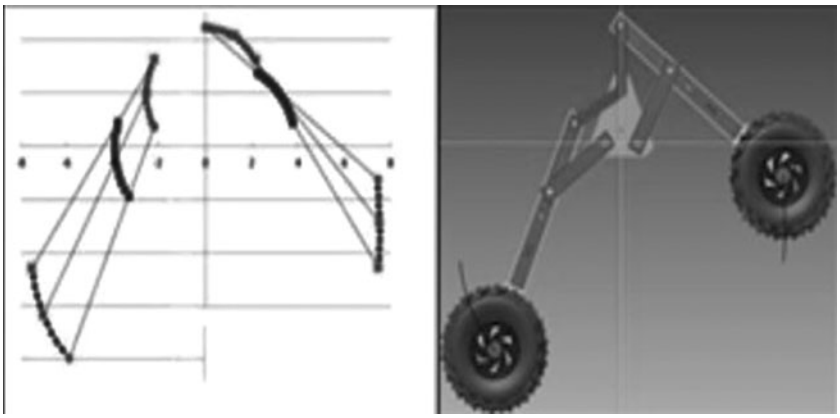

Fig. 8. Passive Rover Suspension front and rear wheel trajectory traced.

Fig. 9. Prototype of the rover at NASA Johnson Space, Houston.

https://doi.org/10.1017/S0263574715000272 Published online by Cambridge University Press

Table V. Task data for the synthesis of the RR chains, used in the design of the mechanical thumb. The angles are measured in radians, the position data is given in units, where 1unit = 1.5 cm.

Posit	$(\phi,\ \boldsymbol{d}_x,\ \boldsymbol{d}_y)$	Vel. Data	Accel. Data
1	(0.2, 2, 1.5)	(1.2, 0.5, 2.09)	–
2	(0, 2.5, 2.5)	(0, 1.18, 4.63)	(1, 0.33, −1)

Table VI. The two real solutions (1unit = 1.5 cm) from the synthesis of the RR chain are gathered together to obtain a one degree of freedom four bar linkage.

Solution	B = (u, v)	P = (x, y)
1	(−0.82, 2.58)	(0.62, 1.59)
2	(0.56, 1.14)	(0.94, 0.45)

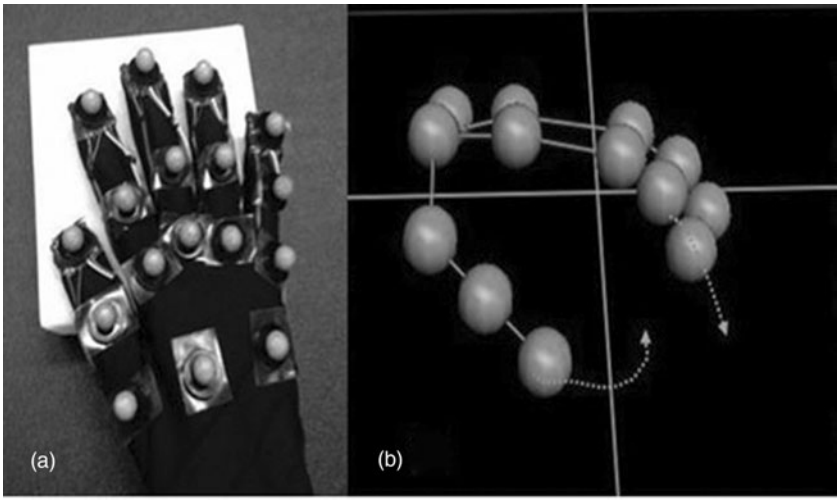

Fig. 10. (a) A prototype of the glove used to obatin experimental data, (b) A screenshot from the motion capture system during grasping task.

complete information about the grasping task. The data is then used to define the position, velocity and acceleration task poses for the kinematic synthesis of the thumb and index fingers. In particular, we chose two task specifications such that PV_1 defines the position and velocity pose on the onset of flexion and PVA_2 defines the position, velocity and acceleration of the fingertip within the vicinity of the contact with an object.

Our design methodology proceeds as follows. We first size the links of the planar 2R serial chain, which we refer as to the "backbone chain," based on human finger dimensions to ensure that the workspace approximate actual finger movements during these two poses. Each of the links l_1, l_2 define the dimensions of the proximal and distal phalange respectively. Next we add another 2R chain to yield a single degree of freedom 4R linkage that moves through the two specified poses. The task for the design of the mechanical thumb is listed in Table V.

The synthesis results are given in Table VI.

For the index finger design, we first size the links of a planar 3R serial chain, which we refer as to the "backbone chain," based on human finger dimensions to ensure that the workspace approximate actual finger movements during these two poses. Each of the links l_1, l_2 and l_3 defines the dimensions of the proximal, middle and distal phalange respectively. Next we add another 3R chain to yield a parallel 3R robot that moves through the two specified poses. Inverse kinematics analysis of the resulting 3R parallel robot yields the configuration of the chain in each of the two poses, which allows us to determine the relative positions, velocity and acceleration of any pair of links in the chain. These

https://doi.org/10.1017/S0263574715000272 Published online by Cambridge University Press

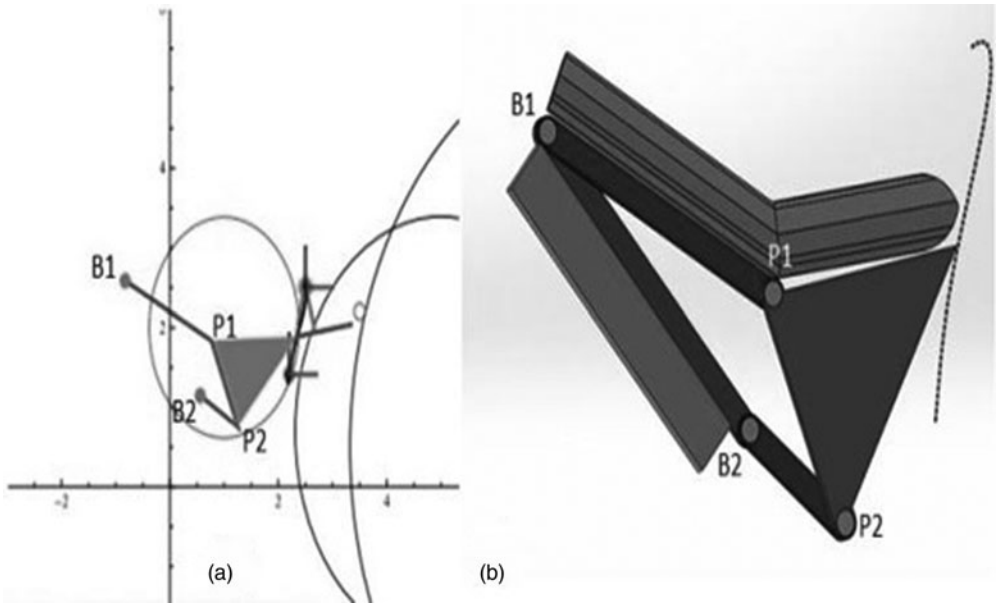

Fig. 11. (a) The four bar linkage used for thumb design in first position, (b) A CAD model of the thumb linkage.

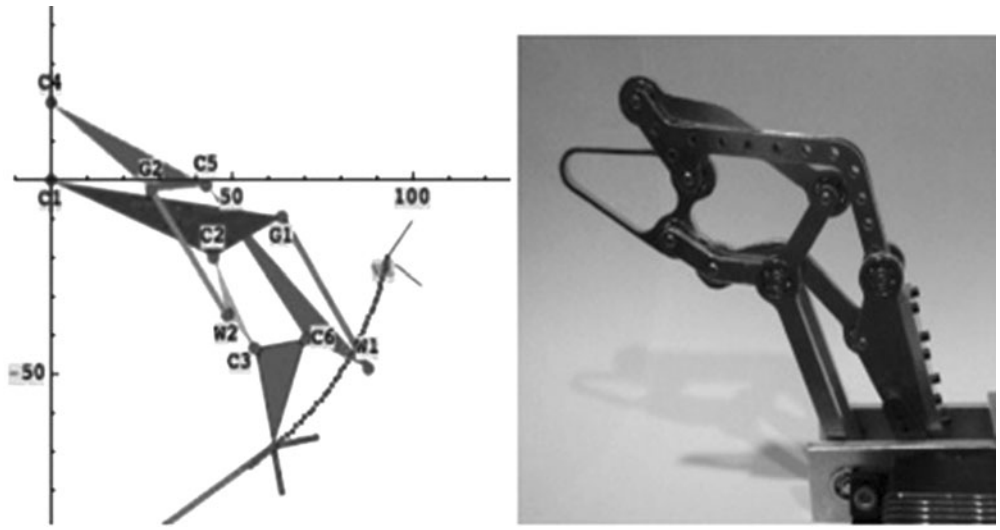

Fig. 12. The mechanical index finger, reaching the specified task with first and second order task constraints, as well as its prototype.

matrices then form the basis for the dimensional synthesis of two RR constraints to obtain a single degree-of-freedom planar eight-bar mechanical device.[16,19] The synthesized index finger is shown in Fig. 12.

Position control of the prototype was chosen for simplicity. A high torque hobby servo allowed for a quick actuation solution to test controlled movement of the linkage. The servo was controlled from Matlab using serial commands written to a servo controller.

6. Summary

This paper considers the synthesis and applications of planar open and closed-loop chains that guide a rigid body such that it does not violate normal direction and curvature constraints imposed by contact with objects in the environment. We define these constraints either by using motion capture system and sensor-based devices, or by transforming the contact direction and curvature constraints

https://doi.org/10.1017/S0263574715000272 Published online by Cambridge University Press

into conditions on the velocity and acceleration of certain points in the moving body, using the task geometry. These motion constraints provide position, velocity and acceleration synthesis equations, which can be solved in order to obtain the desired kinematic chain. Our synthesis procedure was implemented using Mathematica software and requires about 20s to compute the results on a 2.7 GHz Intel Core i7 MacBook Pro.

Future work includes incorporating computer vision techniques for contact point detection, in cases where the bodies have complex geometry and the contact points are *a priori* unknown. These novel techniques will assist not only in choosing the contact points, but also in defining the curvature at these points. Further, the application of the synthesis technique to cases with multiple contacts will be considered. Our preliminary results show that when a hand grasps and object, the constraints on the relative motion among fingers need to be taken into account and the kinematic topology is switching from a tree to a hybrid topology. Lastly, the approach will be extended to the synthesis of spatial kinematic chains. Our pilot results show that the theory can be successfully extended to spherical kinematic chains, such as serial spherical RR and SS chains, as well as spherical four-bar linkages. For spatial complex systems with more degrees of freedom, defining a single velocity might not ensure the desired motion restriction. For example, in the design of multi-fingered robotic hands for manipulative tasks, it is interesting to see if the hand can be designed for a certain manipulative action while keeping the contact with the object and possible force closure in the grasp. Our preliminary results show that given the force closure and mobility conditions, the necessary velocities can be obtained at each task position to fully define a subspace of velocities. This new type of finite *n*th order dimensional synthesis ensures that the motion will be kept in the desired directions. This could be further applied for guiding a grasped object through constrained environments.

Acknowledgements

The authors gratefully acknowledge the assistance of Texas Aggie Mechanical Crutch team at TAMU and the Passive Assistive Walking Device team at CSUF, as well as the support of NSF Grant, Award Id: IIS-1208412, sub-award Id: 2013–2908.

References

1. N. Robson and J. M. McCarthy, "Kinematic Synthesis with Contact Direction and Curvature Constraints on the Workpiece," *ASME International Design Engineering Conference*, Las Vegas, NV, vol. 8, pp. 581–588 (2007).
2. Z. Vafa and S. Dubowsky, "On the Dynamics of Manipulators in Space using the Virtual Manipulator Approach," *Proceedings of the 1987 IEEE International Conference on Robotics and Automation,* Raleigh, NC, vol. 4, 304 (1987).
3. E. Rimon and J. W. Burdick, "A configuration space analysis of bodies in contact - I: 1st order mobility," *Mech. Mach. Theory* **30**(6), 897–912 (1995).
4. E. Rimon and J. W. Burdick, "A configuration space analysis of bodies in contact - II: 2nd order mobility," *Mech. Mach. Theory* **30**(6), 913–928 (1995).
5. D. Tesar and J. W. Sparks, "The generalized concept of five multiply separated positions in coplanar motion," *J. Mech.* **3**(1), 25–33 (1968).
6. H. J., Dowler, J. Duffy and D. Tesar, "A generalized study of four and five multiply separated positions in spherical kinematics–II," *Mech. Mach. Theory* **13**, 409–435 (1978).
7. P. Chen and B. Roth, "Design equations for the finitely and infinitesimally separated position synthesis of binary links and combined link chains," *ASME J. Eng. Ind.* **91**, 209–219 (1969).
8. C. Innocenti, "Polynomial solution of the spatial burmester problem," *J. Mech. Des.* **117**(1), 64–68 (1995).
9. Q. Liao and J. M. McCarthy, "On the seven position synthesis of a 5-SS platform linkage," *ASME J. Mech. Des.* **123**, 74–79 (2001).
10. J. M. McCarthy and B. Roth, "The curvature theory of line trajectories in spatial kinematics," *ASME J. Mech. Des.* **103**(4), 718–724 (1981).
11. J. M. McCarthy and B. Roth, "The instantaneous properties of trajectories generated by planar, spherical and spatial rigid body motion," *ASME J. Mech. Des.* **104**(1), 39–50 (1982).
12. J. M. McCarthy, "Planar and spatial rigid motion as special cases of spherical and 3-spherical motion," *ASME J. Mech. Transm. Autom. Des.* **105**(3), 569–575 (1983).
13. J. M. McCarthy, *Geometric Design of Linkages*, (Springer-Verlag, New York, 2000).
14. J. M. McCarthy, *An Introduction to Theoretical Kinematics*, (The MIT Press, Cambridge, Massachusetts, 1990).

15. N. Robson and A. Tolety, "Geometric Design of Spherical Serial Chains with Curvature Constraints in the Environment," *ASME International Design Engineering Technical Conference*, Washington DC (2011).
16. J. M. McCarthy and G. S. Soh, *Geometric Design of Linkages, Second Edition*, Interdisciplinary Applied Mathematics, (Springer Verlag, New York, 2010).
17. N. Robson, S. Ghosh and G. S. Soh, "Development of a Sensor-Based Glove Device for Extracting Human Finger Motion Data used in the Design of Minimally-Actuated Mechanical Fingers," *3rd IFToMM International Symposium on Robotics and Mechatronics*, Singapore (Oct. 2–4, 2013).
18. G. S. Soh and N. P. Robson, "Kinematic Synthesis of Minimally Actuated Multi-Loop Planar Linkages with Second Order Motion Constraints for Object Grasping," *ASME Dynamic Systems and Control Conference*, Stanford, USA (2013).
19. N. Robson, J. Allington and G. S. Soh, "Development of Under-actuated Mechanical Fingers based on Anthropometric Data and Anthropomorphic Tasks," *ASME International Design Engineering Technical Conference*, Buffalo, NY (2014).

https://doi.org/10.1017/S0263574715000272 Published online by Cambridge University Press